Int. J. of Thermodynamics
ISSN 1301-9724

Vol. 12 (No. 4), pp. 193-202, December 2009
www.icatweb.org/journal.htm

# Turbocharger Heat Transfer Modeling Under Steady and Transient Conditions

Mickaël Cormerais[1], Pascal Chesse[2], Jean-François Hetet[3,]*

Internal Combustion Engine Team, Laboratory of Fluid Mechanics, UMR 6598 CNRS
Ecole Centrale de Nantes, BP 92101,44321 Nantes Cedex 3, France
E-mail: [1]mickael.cormerais@ec-nantes.fr, [2]pascal.chesse@ec-nantes.fr, [3]Jean-Francois.hetet@ec-nantes.fr

**Abstract**

In the field of automotive propulsion, environmental issues (need for drastic reduction of greenhouse gases) and diminishing fossil fuels supplies enhance the need to reduce fuel consumption. To reach this goal, a possible solution is downsizing. Unfortunately, the degradation of the transient performance of the engine limits the expected benefits of downsizing. Engine manufacturers try to improve turbocharger matching using simulation. However, the literature and experiments on a turbocharger test bench show that, contrary to general opinions, heat transfer can influence the turbocharger performance. Thus it seems essential to determine and correlate the different types of heat transfer phenomena occurring in a turbocharger. First a complete experimental characterization of turbocharger heat transfer is performed in steady and transient conditions. The experimental results are used to correlate turbocharger heat transfer coefficients. Then, the equivalent heat transfer resistance method is explained. The correlations obtained are then used in this method to calculate all heat transfer interactions within the turbocharger and transferred to the surroundings in steady and transient conditions. In each case, comparisons between numerical and experimental results are performed to verify the quality of the method proposed.

***Keywords:*** *Turbocharger, heat transfer, heat resistance*

## 1. Introduction

In the field of automotive propulsion, environmental issues (drastic reduction of greenhouse gases) and diminishing fossil fuels supplies enhance the need of fuel consumption reduction. To reach this goal, it is possible to increase the engine specific power at constant rotational speed (downsizing). The degradation of the transient performance of the engine limits the expected benefits of downsizing. Engine manufacturers try to improve turbocharger matching using simulation codes. An analysis of the models included in those codes shows that the turbochargers performance calculations are based on a simple interpolation in the turbochargers maps. In that case, the major assumption is that compression and expansion are adiabatic. For highly turbocharged engines, experiments on test bench show that this assumption is not acceptable (Cormerais et al., 2006a; Cormerais, 2007). Indeed, a significant amount of heat is transferred through the surface, the flanges, and the bearing oil and a significant part is transferred from the turbine to the compressor. These heat transfers can influence the turbocharger performance (Rautenberg and Kammer, 1984; Jung et al., 2002; Bohn, 2003a; Cormerais et al., 2006b). As a consequence, simulation codes provide inaccurate results for certain operating points.

Thus, it appears essential to quantify and then to model heat transfer occurring in a turbocharger to accurately simulate the dynamic behavior of the engine. The scope of this work is to propose a method to "calculate the heat transfers" occurring in a turbocharger from geometric data.

## 2. Bibliography

Various studies have already stated the need of a non-adiabatic approach for the turbocharger. The first detailed analysis on heat transfer incidences on the turbocharger performances was presented in 1984 by Rautenberg et al. (Rautenberg et al., 1984; Rautenberg et al., 1986). Based on an experimental study, they showed that the compression and expansion processes are not adiabatic. Part of the power yielded by gases in the turbine is transferred to the surroundings, to the bearing housing and finally to the compressor. Moreover, the authors showed that the turbine measured non-adiabatic efficiency is not an aerodynamic quality measurement of the expansion process. They then proposed a method to calculate the turbine and compressor adiabatic efficiencies from a phenomenological study and the efficiencies obtained during the hot tests.

Jung et al. (Jung et al., 2002; Jung, 2003) affirmed that at low rotational speed and mass flows, heat transfer via the turbocharger housing affect the efficiency calculated from the temperature measurements. To calculate the actual efficiency, they suggested a parameterization of the turbine maps in separating the aerodynamic efficiency and the increase in the efficiency due to heat transfer. The heat efficiency was calculated considering the turbine as an exchanger whose efficiency depends on the mass flow.

Chapman et al. (2002) studied the heat transfer effects on turbocharger performance. First of all, the authors carried out tests on a water-cooled turbocharger to obtain heat transfer coefficients and the boundary conditions for CFD studies. In order to determine the transfers in oil and water, the authors analyzed the experimental results by carrying out the energy balance of each fluid. The heat transfer study was followed by a turbocharger CFD modeling. This study seemed to indicate that water and oil are heat barriers that strongly decrease any transfer between the turbine and the compressor. Finally, the use of the experimental and numerical results made it possible to obtain the values of all the heat transfers considered. In conclusion, the authors gave an expression for the turbine and compressor isentropic efficiencies for a non-adiabatic transformation. The efficiencies thus corrected are largely different from the ones measured.

*Corresponding Author

Using the work of Rautenberg et al. (1986) 17 years afterwards, Bohn et al. (Bohn, 2003a; Bohn, 2003b; Bohn at al. 2005) investigated turbocharger heat transfer in developing a 3-D conjugate calculation simulation including the compressor, the oil cooled centre housing, and the turbine. The aerothermal and heat boundary conditions needed were obtained by experiments (Bohn, 2003b). These experimental results made it possible as well to carry out a qualitative analysis of the heat transfer between the turbine and the compressor. This study showed among others that the radiative transfer between turbine and compressor housings is negligible. Finally, the numerical simulation provided heat transfer distribution within the turbocharger, and it allowed a parametric study with variations of the mass flows and the turbine inlet temperature. Finally a heat transfer correlation was proposed.

Shaaban (Shaaban, 2004; Shaaban and Seume, 2006) indicated that it is necessary to quantify heat transfer within turbochargers. Shaaban (2004) thus proposed a diagram of the various turbocharger heat transfers and powers where the convective and radiative heat transfers between the turbine and compressor scrolls, and the heat losses from the compressor to the surroundings are neglected. The author thus calculated all the heat transfer coefficients by carrying out a turbocharger energy balance. He showed that heat transfer to the surroundings accounts for 70% of the total heat power lost by the turbine. The heat power transferred to the compressor accounts for only 10%. Finally, the author showed that the total heat power can reach 8 times the turbine mechanical power at low rotational speeds and small flows. Once all heat transfers were quantified, modeling was performed. For this purpose, he maked the assumption that all heat transfers were in the same direction which enabled the use of a 1-D method. The method consisted of applying the conservation equation of energy to an element *dx* of the turbocharger housing in steady conditions. From the boundary conditions, experimental results and some simplifications, the author proposed empirical expressions for heat transfer.

Baar et al. (2005) showed that most driving code does not take into account heat transfer in the turbocharger. Consequently, important discrepancies occured with the experimental results especially at low engine load. Then to quantify all the turbocharger powers and heat transfers, they propose a summary diagram from which they carry out the complete energy balance of this turbocharger. Baar et al. (2005) concluded on the fact that the equations obtained can be solved from the experimental results of the adiabatic and non-adiabatic tests. Hagelstein et al. (1999) also used an equivalent diagram in order to define the various powers concerned and to calculate them. However the exact method was not explained in detail. The equations were not given explicitly.

In complement, one can quote the works of Podevin et al. (2002) and Pucher et al. (2005) that study the influence of oil properties on turbocharger performance and more particularly on compressor performance.

The aforementioned studies can be regarded as the most significant works on heat transfer within turbochargers. Other research work (Lallemand, 1983; Younes, 1993; Descombes, 1996; Gayvallet et al., 1987) evoked this subject, but they failed to provide any decisive elements. Other papers on heat transfer in gas turbines exist. For example, we can quote the works of Moreno-Salas (2006), Khalid and Hearne (1980), Larjola (1982), Riegler (1999), Guzovic et al. (2001), Senechal (1994), and Jones (1991). But, the results of these are not directly useable in this study.

## 3. Experiments

Most research works presented in the previous part use experimental results to study heat transfer within a turbocharger.

### 3.1. Turbocharger Test Bench

The experimental facility is a steady flow turbocharger test bench with hot air located at the Laboratory of Fluids Mechanics of the Ecole Centrale de Nantes. A complete description of this facility has been presented elsewhere (Cormerais, 2007). Figure 1 shows a schematic diagram of the test bench.

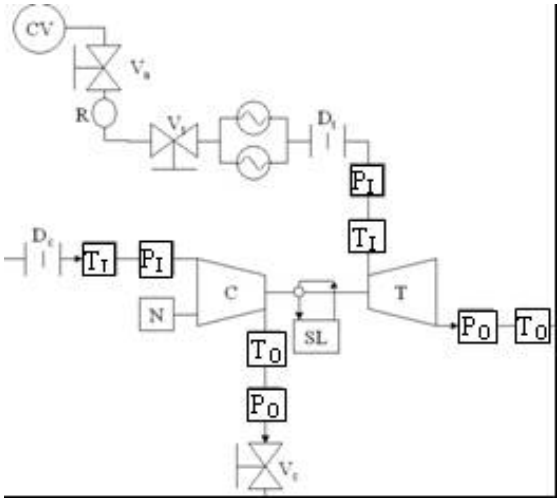


*Figure 1. The Turbocharger Test Bench.*

The screw compressor (CV) provides the compressed air at a maximum pressure of 7 bars and a maximum air flow of 1200 $Nm^3/h$. The electric air heaters allow the regulation of the turbine inlet temperature ($T_{ET}$) varying from 300K to 900K. An oil pump (SL) lubricates the turbocharger. This turbocharger test bench allows measuring the turbine ($T_{ET}$, $T_{ST}$), compressor ($T_{EC}$, $T_{SC}$) and oil ($T_{EH}$, $T_{SH}$) inlet and outlet temperatures with thermocouples. The turbine ($P_{ET}$, $P_{ST}$) and compressor ($P_{EC}$, $P_{SC}$) inlet and outlet pressures are measured with piezoresistive sensors, and oil inlet and outlet pressures with pressures gauges. The turbocharger speed (N) is measured with an inductive sensor. The compressor ($D_C$) and turbine ($D_T$) air mass flows are measured with orifice plates. All these measurements are registered by a data acquisition system and the evolution of these measurements is monitored on a PC screen.

### 3.2. Phenomenological Analysis

The results of the phenomenological analysis carried out on a turbocharger are represented in Figure 2. A part of the turbine power is lost by convection to the bearing housing "$\dot{Q}_T$" and to the surroundings by natural convection and radiation. The other part "$\dot{W}_T$" is transferred to the shaft. The heat transfer from the turbine to the bearing housing "$\dot{Q}_T$" is divided into a transfer to the oil "$\dot{Q}_H$", a transfer to the compressor "$\dot{Q}_C$" and a transfer to the surroundings. A part of the mechanical power "$\dot{W}_T$" is lost by friction in

bearings "$P_F$". The other part "$\dot{W}_C$" is transferred to the compressor gases. A part of the compressor power is lost to the surroundings.

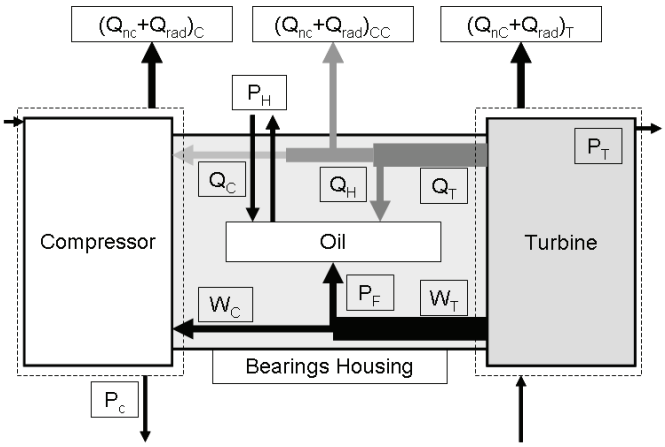


*Figure 2. Turbocharger Powers.*

### 3.3. Steady Experiments

The goal of the experiments is to obtain all the power and heat fluxes represented in

Figure 2. Four kinds of experiments are performed on the turbocharger test bench; three experiments in steady, one in transient condition. The first three experiments in steady condition consist of measuring a number of constant speed lines on the compressor and the turbine characteristics maps. The constant speed lines correspond to corrected speeds between 60000 and 155000 rpm. The first two experiments are performed to characterize and correlate the different heat transfers occurring within the turbocharger. For this purpose, the turbocharger being tested is insulated with a blanket of alkaline earth silicate wool composed of calcium, magnesium and silicate. The power transferred from the turbocharger to the surroundings is thus neglected. The third kind of experiment is used to calculate heat transfer to the surroundings.

#### 3.3.1. Insulated, Adiabatic Tests

The first experiment corresponds to an adiabatic compression process. The turbine inlet temperature is regulated to have the average temperature of the fluid crossing the turbine equal to that of the fluid crossing the compressor. Consequently there is no significant heat transfer within the turbocharger. The turbine and the compressor are thus considered adiabatic. To analyze the experimental results, the energy balances of each part of the turbocharger are made. On the basis of perfect gas assumption, this analysis allows obtaining the turbine ($\dot{W}_T$) and compressor ($\dot{W}_C$) mechanical powers and the power lost by friction ($P_F$), the turbine ($\eta_{T_{IS}}$) and compressor ($\eta_{C_{IS}}$) isentropic efficiencies and the mechanical efficiency ($\eta_m$).

$$\dot{W}_C = \dot{m}\left(\frac{\dot{Cp}_{IC} + Cp_{OC}}{2}\right)(T_{OC} - T_{IC}) \quad (1)$$

$$\dot{W}_T = \dot{m}\left(\frac{\dot{Cp}_{IT} + Cp_{OT}}{2}\right)(T_{IT} - T_{OT}) \quad (2)$$

$$P_F = \dot{W}_T - \dot{W}_C \quad (3)$$

$$\eta_{C_{IS}} = \frac{\dot{W}_{C\,IS}}{\dot{W}_C} \quad (4)$$

$$\eta_{T_{IS}} = \frac{\dot{W}_T}{\dot{W}_{T_{IS}}} \quad (5)$$

$$\eta_m = \frac{\dot{W}_C}{\dot{W}_T} \quad (6)$$

#### 3.3.2. Insulated, Non-adiabatic Tests

The second experiment carried out consists of regulating the turbine inlet temperature from 200°C to 500°C in steps of 100°C. The turbocharger is still insulated. To analyze the experimental results, the energy balances of each part are carried out. These assessments make it possible to obtain the transfer of the turbine to the bearing housing ($\dot{Q}_T$), from the bearing housing to the compressor ($\dot{Q}_C$) and the oil ($\dot{Q}_H$). The compressor mechanical power ($\dot{W}_C$) is calculated thanks to the isentropic efficiency map measured previously. This method is not transposable with the turbine mechanical power because the measured zone is too narrow. It is thus necessary to know the friction power ($P_F$) to solve the system of equations.

Thus the first test is also used to correlate the friction power. To obtain this result, the formulation considered is based on the hydrodynamic bearing theory. The charge is considered as a linear combination of the average turbine and compressor gases pressures. The formulation used is:

$$W_F = a.\mu^b.N^{1+b}.(P_{IT} + c.P_{OC})^{1-b} \quad (7)$$

where a, b, c are correlation constants which are obtained by an optimization software ModeFrontier (Esteco, 2009) using a genetic algorithm and experimental results of the adiabatic and insulated test. This correlation is used in the non-adiabatic test analysis to obtain the turbine mechanical power and then all the powers.

#### 3.3.3. Non insulated, Non-adiabatic Tests

For this test, the turbocharger is not insulated any more. The turbine inlet temperature is regulated from 200°C to 500°C by step of 100°C Furthermore seven additional thermocouples are fixed on the walls. The purpose of this test is to quantify the heat losses to the surroundings.

### 3.4. Transient Experiment

The last experiment carried out consists of a linear increase of the turbine inlet temperature from 100°C to 200°C. The valve positions are not changed during this transient operation. The origin operating point is on the corrected compressor constant speed line 310 m/s. The 7 wall temperatures are still measured. The experimental results obtained have been used to test the numerical results of the transient equivalent heat resistance method (Cormerais, 2007).

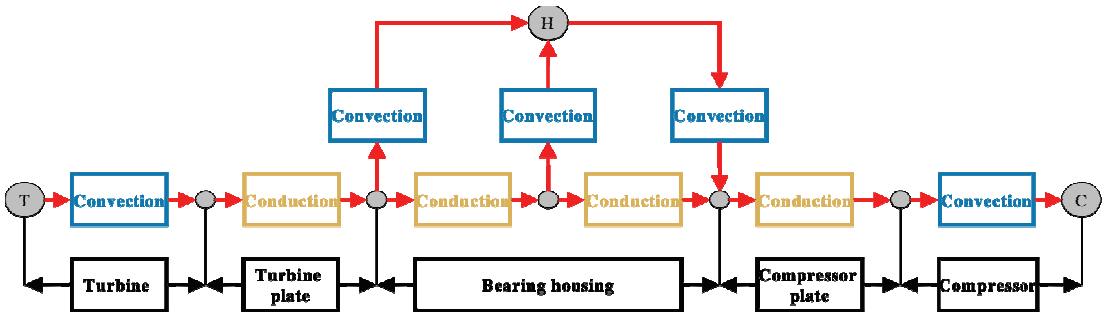


*Figure 3. Configuration of Turbocharger Heat Transfer Resistances.*

## 4. Equivalent Heat Transfer Resistance Method (EHTR Method)

### 4.1. Presentation

This method consists of associating each heat transfer Q by its equivalent heat transfer resistance R. Equivalent resistance is defined by Eq. (8).

$$R = \frac{\dot{Q}}{\left(T_X - T_{wo}\right)} \tag{8}$$

where $T_X$ is the inlet wall temperature of the part considered or a fluid temperature in contact. And $T_{WO}$ is the outlet wall temperature or the wall temperature in contact with a fluid.

To be able to use these resistances, several assumptions must be made. First of all the distribution of the temperatures in the radial and tangential directions must be considered uniform. Moreover, it is considered that the oil entirely fills the interstices of the bearing housing.

To use equivalent resistance related to a conductive heat transfer, the conductivity and the section of each part must be constant. Thus the turbocharger must be divided in parts chosen to take into account heat transfer significant surfaces and to have the most constant possible section. However the different selected parts can have different sections. As depicted in Figure 4, the turbocharger is divided in five parts: two scrolls, two plates and the bearing housing.

It must be noted that the heat transferred within the shaft has been included in the total heat transfer from the turbine to the bearing housing ( $\dot{Q}_T$ ) or from the bearing housing to the compressor ( $\dot{Q}_C$ ).

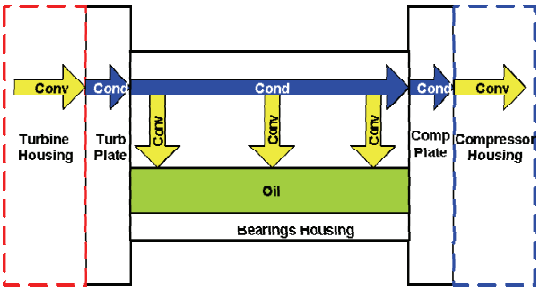


*Figure 4. Turbocharger Parts and Related Heat Transfers.*

Figure 3 shows the heat resistance configuration considered for an insulated turbocharger. This configuration can be simplified with only three resistances defined in relation to the various convective and conductive heat transfer coefficients as indicated in Figure 5. To obtain this last configuration, a calculation of equivalent resistances is carried out starting from the basic Kirchoff's laws.

Once this configuration obtained, the three heat transfers ( $\dot{Q}_T$ , $\dot{Q}_H$ , $\dot{Q}_C$ ) considered for the experiments can be formulated in a simple way in relation to the turbine; compressor and oil inlet temperatures (Eqs. (9), (10), and (11)).

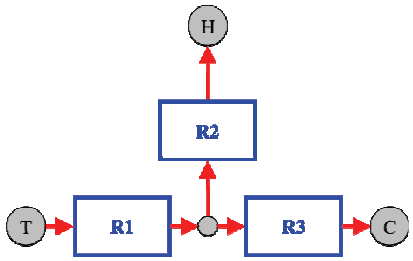


*Figure 5. Configuration of Final Heat Transfer Resistances.*

$$\dot{Q}_T = \frac{\left(T_T\left(R_2+R_3\right) - R_3.T_C - R_2.T_H\right)}{R_1.R_2 + R_2.R_3 + R_3.R_1} \tag{9}$$

$$\dot{Q}_H = \frac{\left(T_T.R_3 + R_1.T_C - \left(R_3+R_1\right).T_H\right)}{R_1.R_2 + R_2.R_3 + R_3.R_1} \tag{10}$$

$$\dot{Q}_C = \frac{\left(T_T.R_2 + R_1.T_H - \left(R_1+R_2\right).T_C\right)}{R_1.R_2 + R_2.R_3 + R_3.R_1} \tag{11}$$

### 4.2. Nusselt Number Correlation

The use of a direct method to obtain the convective heat transfer coefficients is not possible in a simple way. An implicit method is thus used. It consists of giving a form for the correlations of these coefficients based on the Nusselt number. The constants introduced are optimized in order to obtain values of heat transfers in good agreement with the experimental results.

For the compressor, most of the heat transfer probably appears after the rotor. However, the flow conditions in the diffuser and the volute are dependent on the turbocharger rotational speed. It is thus necessary to take into account this parameter in the correlations. For the turbine, the heat transfer to the bearing housing appears mainly upstream of the rotor. So, the rotational speed does not influence the turbine heat transfers. To simplify the study, the constants to be optimized are limited. Thus, it was selected to set the exponent of the Prandt number and of the Reynolds number depending on the mass flow with the values suggested by Depcik and Assanis (2002). With regards to the transfer between oil and the bearing housing, the correlation is

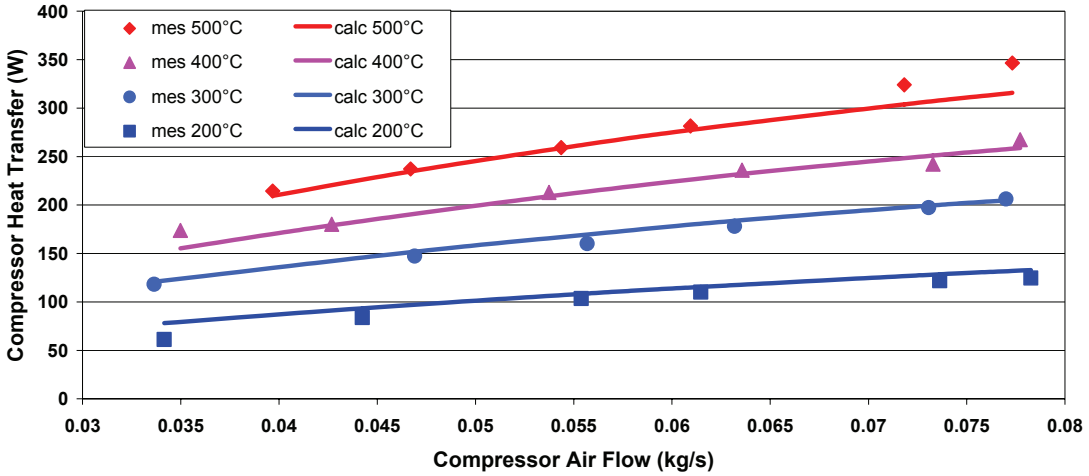


*Figure 6. Calculated and Measured Compressor Heat Transfer.*

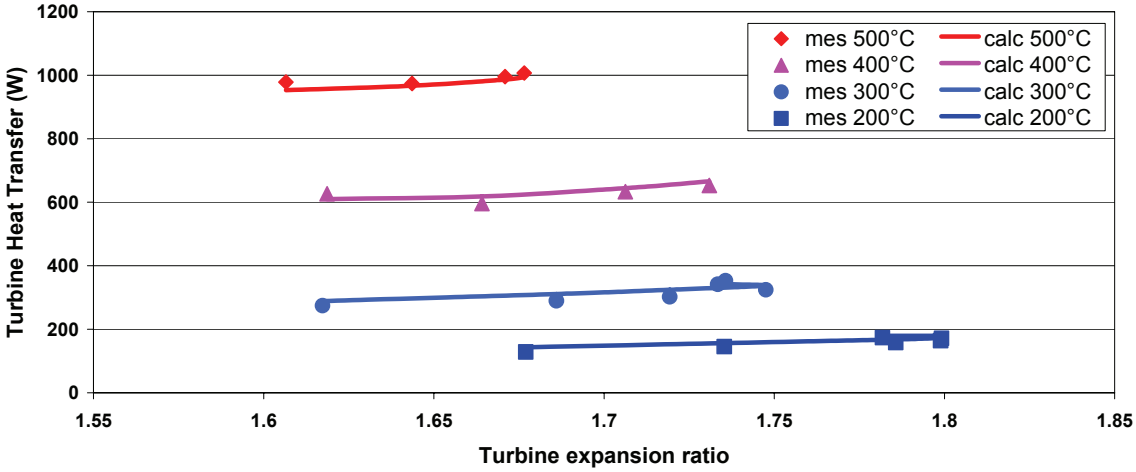


*Figure 7. Calculated and Measured Turbine Heat Transfer.*

based on work of Busam et.al. (2000). The constant values are obtained using optimization software (ModeFrontier (Esteco, 2009)), which uses a genetic algorithm and the non-adiabatic and insulated test experimental results. The three correlations obtained are:

$$\text{Considering, } \mathrm{Re} = \frac{4\dot{m}}{\mu\pi D} \tag{12}$$

$$\text{and } \mathrm{Re}_u = \frac{\rho\left(\frac{\pi DN}{60}\right)D}{\mu} \tag{13}$$

$$Nu_c = 3{,}16.10^{-6}\,\mathrm{Re}^{0.75}\,\mathrm{Re}_u^{0.58}\,\mathrm{Pr}^{1/3} \tag{14}$$

with $D = \sqrt{4.L.D_{ext}}$ , where

L is the blade width at wheel exit and $D_{ext}$ is the extern wheel diameter.

$$\mathrm{Nu_T} = 0.14.\mathrm{Re}^{0.75}.\mathrm{Pr}^{1/3} \tag{15}$$

with $D = \sqrt{4.L.D_{ext}}$ , where

L is the blade width at wheel inlet $D_{ext}$ is the extern wheel diameter.

$$\mathrm{Nu_H} = 4.81.10^{-5}.\mathrm{Re}^{0.8}.\mathrm{Re_u}^{0.35} \tag{16}$$

with $D = \sqrt{D_{ext\_shaft}^2 - \Phi_{\mathrm{int}}^2}$ , where

$D_{ext\_shaft}$ is the axis extern diameter and $\Phi_{\mathrm{int}}$ is the axis intern diameter.

Turbocharger heat transfers are calculated with the formulations and the correlations obtained with the equivalent heat transfer resistance method. These values are compared with the experimental results for the 4 turbine inlet temperatures and the 3 corrected rotational speeds tested during the non-insulated non-adiabatic experiment. But only one corrected speed line (128000 rpm) is shown for the compressor (Figure 6) and for the turbine (Figure 7). The oil heat transfer can be obtained from the 2 first transfers.

The results obtained from the correlations established previously correspond well to the experimental results for the turbine and the compressor heat transfers. The main errors are obtained for a turbine inlet temperature equal to 500°C. For all operating points tested, the average relative error is lower than 3.5% for the turbine and 5.5% for the compressor.

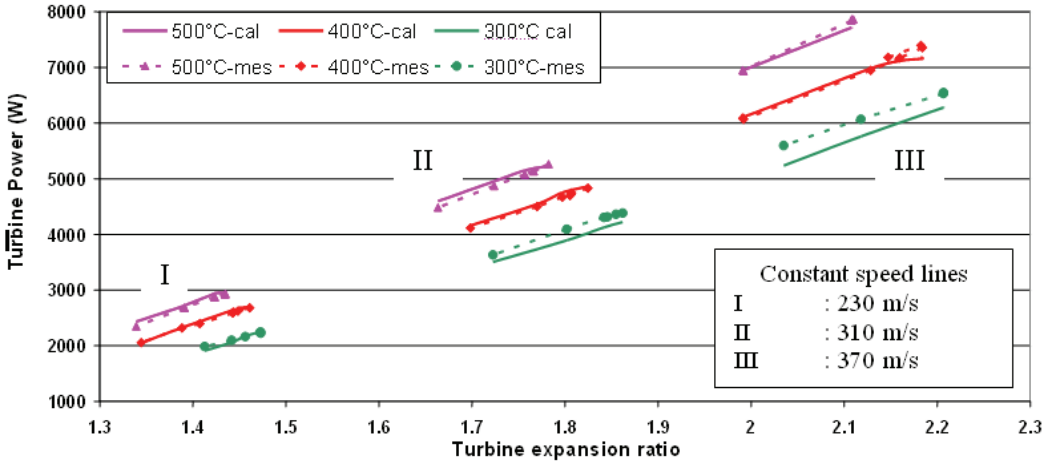


*Figure 8. Calculated and Measured Total Turbine Power.*

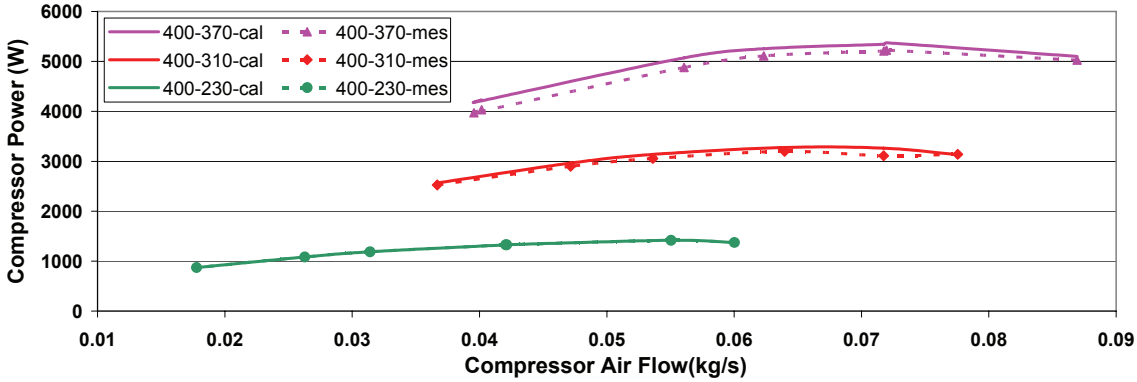


*Figure 9. Calculated and Measured Total Compressor Power.*

### 4.3. Heat transfer to the Surroundings

The power lost to the surroundings could not be measured directly. Indeed, these power losses influence the total turbocharger energy balance. Consequently, the differences between the powers calculated from the inlet and outlet temperatures (total powers) with or without insulator are not equal to the powers lost to the surroundings.

A possible method to solve this problem is to consider a heat transfer resistances configuration of a non-insulated turbocharger. This configuration has to represent all the heat transfers to the surroundings. A first difficulty is then to know to which nodes the losses must be applied. Once the configuration is obtained; it is very complicated to simplify it in the form of three equivalent resistances. So it is difficult to find a simple formulation for all heat transfers. A numerical resolution can be considered, but that does not correspond to our purpose. Thus this method is not studied in greater detail.

First of all, it is very important to note that heat is mainly lost by natural convection and radiation to the surroundings in the turbine and compressor scrolls. So a simple method to take into account these losses in a calculation is to consider that they act as first in the scroll and a new turbine inlet temperature is calculated. Then the transfer within the turbocharger is taken into account by using the previous formulations, correlations and the new calculated temperature. Finally, the expansion is considered, the mechanical powers are calculated from the adiabatic test measures. For the compressor, the method is simply the inverse of the one used for the turbine. First of all, compression is considered, and then the heat transferred from the bearing housing is taken into account. Finally the compressor outlet temperature is decreased because of the heat losses to surroundings.

After some tests, the Nusselt number correlation proposed by Sacadura (1993) is used to calculate the natural convection coefficient (Eq. 17).

$$\text{If}\left(Pr.Gr\right) < 10^9$$

$$Nu = 0.53.\left(Pr.Gr\right)^{0.25} \qquad (17)$$

Else

$$Nu = 0.13.\left(Pr.Gr\right)^{0.33}$$

The heat transfer by natural convection is calculated by Eq. (18).

$$\dot{Q}_{nc} = h_{sur}.A_{sur}.\left(T_w - T_{sur}\right) \qquad (18)$$

The heat transfer by radiation is calculated using the Eq. (19).

$$\dot{Q}_{rad} = \varepsilon_w.\sigma.A_{sur}.\left(T_w^4 - T_{sur}^4\right) \qquad (19)$$

where $\sigma$ is the Stefan-Boltzmann constant.

The wall emissivities measured by Bohn et al. (2005) are used for this calculation. The wall temperatures required for these calculations are directly the measures realised on the turbocharger test bench. Figure 8 shows the comparison between the total turbine powers calculated and measured for the three turbine inlet temperatures and constant speed lines tested.

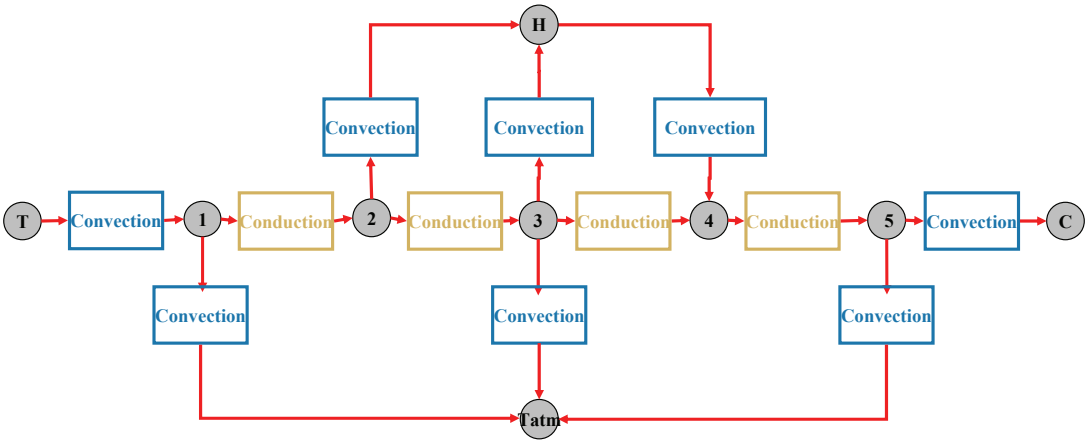


*Figure 10. Configuration and Inertias of Heat Transfer Resistance.*

Figure 9 shows the same comparison for compressor powers. Only one constant speed line is represented but the conclusions are the same for the two other rotational speeds.

The numerical results are in good agreement with the measured powers. However as the rotational speed increases, the difference between the numerical and experimental results increases. For the turbine, the error compared to the experimental results does not exceed 7%, which corresponds to the error found for the internal heat transfers. The maximum deviation is of 300W for a power of 6000 W. For the compressor, the results obtained are in good agreement with measurements. The discrepancy between the calculated and measured powers does not exceed 6%. The maximum deviation is lower than 50 W what accounts for hardly 5% of the total power. Thus, the method proposed allows calculating the power lost to the surroundings in a very good agreement with experimental results.

### 4.4. Heat transfer in Transient Conditions

To use the EHTR method in transient state, it is possible to consider inertia concentration points whose mass correspond to those of the modeled part. As the thickness of these concentrations is very low, the heat transfer is considered equivalent to a Newtonian cooling or heating. Conduction is not directly taken into account in these points. However conduction is considered all the same from a total point of view. It is represented by its heat resistance in steady state. First of all, the method consists of placing these inertia concentrations on the heat transfer configuration considered. Then the energy equation is applied to each concentration. These equations are then solved in order to obtain the values of the inertia concentration point's temperatures. Once these temperatures obtained, it is possible to calculate heat transfers in a turbocharger. The simplest configuration is obtained by considering only one inertia concentration placed at the intersection point of the three equivalent resistances of Figure 5. The energy equation applied to this concentration is:

$$\rho.C.V.\frac{\partial T_{pCI}}{\partial t}=\frac{1}{R_1}\left(T_T-T_{pCI}\right)+\frac{1}{R_2}\left(T_H-T_{pCI}\right)+\frac{1}{R_3}\left(T_C-T_{pCI}\right) \quad (20)$$

This equation is a non-homogeneous one degree differential equation. The virtual temperature is given by the Eq. (21) where the boundary conditions are considered:

$$T_{pCI}=T_0.e^{-\alpha.t}+H\left(1-e^{-\alpha.t}\right) \quad (21)$$

with

$$H=\frac{R_1.R_2.T_C+R_2.R_3.T_T+R_1.R_3.T_H}{R_1.R_2+R_2.R_3+R_1.R_3} \quad (22)$$

$$\alpha=\frac{\frac{R_1.R_2+R_2.R_3+R_1.R_3}{R_1.R_2.R_2}}{\rho.C.V} \quad (23)$$

Theoretically, this solution is correct only if the turbine, compressor and oil inlet temperatures are constant. However during a transient operation, the variations of the compressor and oil temperatures are small, which is not the case for the turbine inlet temperature. However the variations of this temperature are due to pipe filling whose time-constant is low compared to that related to the heat transfer inertia.

The inertia concentration point temperature does not correspond obviously to a measurable physical temperature on the turbocharger. However this method makes it possible to quickly obtain the important heat transfers without having to use numerical methods. To approach as close as possible the real configuration of the turbocharger it is possible to multiply the inertia concentration points in order to better take into account each part considered. Unfortunately, in this case the analytical resolution of the energy equations is not possible any more. Figure 10 shows the heat transfer resistance configuration and the inertia concentration points. Item 1 corresponds to the turbine housing, item 2 with the turbine plate, item 3 with the bearing housing, item 4 with the compressor plate and finally item 5 corresponds to the compressor housing. The five equations allowing the calculation of the inertia concentration point temperatures are in the form:

$$\rho.C.V_i.\frac{\partial T_{pCI^i}}{\partial t}+\left(\frac{1}{R_{i-1}}+\frac{1}{R_i}+\frac{1}{R_{i+1}}\right)T_{pCI^i}=\frac{1}{R_{i-1}}T_{pCI(i-1)}+\frac{1}{R_{i+1}}T_{pCI(i+1)}+\frac{1}{R_i}T_i \quad (24)$$

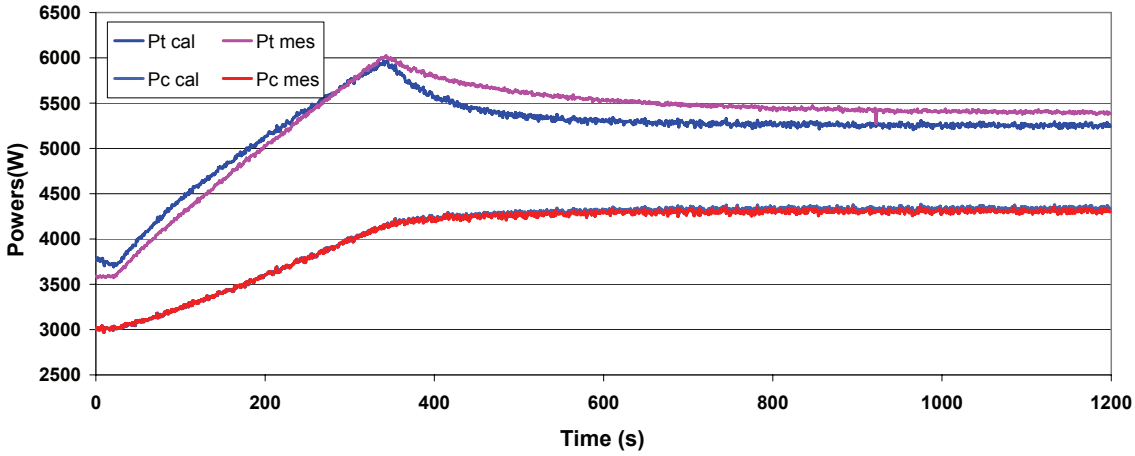


*Figure 11. Calculated and Measured Turbine and Compressor Powers*

Finally, a system of fivr coupled total differential equations is obtained. The heat transfers within the turbocharger result from the following equations:

$$\dot{Q}_T = h_T.A_T.(T_T - T_{P1}) \quad (24)$$

$$\dot{Q}_C = h_C.A_C.(T_{P5} - T_C) \quad (25)$$

$$\dot{Q}_H = h_H.A_{H2}.(T_{P2} - T_H) + h_H.A_{H3}.(T_{P3} - T_H) + h_H.A_{H4}.(T_{P4} - T_H) \quad (26)$$

The convection coefficients necessary to obtain these results are calculated with the correlations obtained in steady state. The heat transfers within the turbocharger and the powers lost to the surroundings are considered in transient calculation. The test showed in Figure 11 is a temperature linear evolution from 100°C to 300°C at the turbine inlet during 300 s. Due to the turbocharger thermal inertia, the turbine power is maximum when the turbine inlet temperature reaches the final temperature of 300°C. Then the turbine power decreases to reach the steady state. The comparison with the experimental results is thus carried out by considering the total turbine and compressor powers. To calculate these results, the experimental turbine and compressor mechanical powers are used in both cases. Thus only heat transfer calculations are compared.

Figure 11 shows the comparison between the numerical and experimental turbine and compressor total powers.

For the compressor, the numerical results are in a very good agreement with measurements. The maximum deviation is only 1.5%. This model respect the evolution of this power, the calculated transient time-constant is close to that measured. It is the same for the turbine. The particular evolution of the turbine total power ($P_T$) is also obtained by calculation with a difference, compared to experimental results, at the maximum value of about 40W. However the end value is not calculated with the same precision. It is obtained with a variation of 130 W, corresponding to an error of 2.5%.

The compressor outlet temperature is obtained with a discrepancy of 2 degrees, which is close to the measure uncertainties. The results are thus in very good agreement with measurements. For the turbine, the difference between the temperatures measured and calculated is almost constant once the rise of the turbine inlet temperature is finished. This variation is of 4°C.

The equivalent heat transfer resistance method makes it possible to calculate the heat transfers within a turbocharger and the heat losses to the surroundings with a very good precision in steady and transient states. Furthermore, most important in the transient case, the model is able to follow the particular evolution of the powers.

## 5. Conclusion

Heat transfer influences the turbocharger performance, especially at low and partial loads. Heat transfer models exist but are generally limited to specific and "badly" definite situations, and mainly during incidence studies of these phenomena on a turbocharger simulation. Thus, the heat transfer modeling must be based on an experimental study.

First of all, the experimental characterization allows, using the adiabatic and insulated tests, to obtain the values of the mechanical powers and the compressor and turbine isentropic efficiencies as well as the correlation of the power lost by friction in oil. Then the non-adiabatic and insulated test analysis allows us to obtain the turbocharger internal heat transfers. The non-adiabatic and non-insulated tests provided the results necessary to the validation of the heat losses to the surroundings models. Finally the test in transient conditions is used to test the turbocharger dynamic behavior modeling.

The equivalent heat transfer resistance makes it possible to calculate the heat transfers within a turbocharger and the heat losses to the surroundings with a very good precision in steady and transient conditions. In this last case, this method allows to calculate turbine and compressor total powers whose evolutions follow those of the experimental values. However the results obtained by this method at the transient end are not in total agreement with measurements. The error on the end value can be strongly decreased by readjusting the heat transfer coefficients. Most important in the case of transient is to be able to follow the evolution of the powers.

This turbocharger heat transfer modeling will be applied to a complete engine simulation in order to solve problems encountered during simulation in particular at low and partial loads. Several boundary conditions will have to be modified in order to take into account the characteristics of the turbocharger driving environment.

**Nomenclature**

| | | |
|---|---|---|
| A | Section | m² |
| Cp | Specific heat at constant pressure | J/kg/K |
| CV | Volumetric Compressor | |
| D | Diameter | m |
| Dc | Compressor flowmeter | |
| Dt | Turbine flowmeter | |
| Gr | Grashoff Number | - |
| h | Convection coefficient | J/kg |
| l | Width | m |
| $\dot{m}$ | Mass flow | kg/s |
| N | Rotational speed | rpm |
| Nu | Nusselt number | - |
| P | Pressure | Pa |
| $P_F$ | Friction losses | W |
| Pr | Prandt number | - |
| $\dot{Q}$ | Heat flow | W |
| R | Heat resistance | W/k |
| r | Gas perfect constant | J/kg/K |
| Re | Reynolds number | - |
| $Re_U$ | Rotational Reynolds number | - |
| SL | Lubricating system | |
| t | Time | s |
| T | Static temperature | K |
| Va | Security valve | |
| Vc | Compressor control valve | |
| Vt | Turbine control valve | |
| $\dot{W}$ | Power | W |

**Greek Letters**

| | | |
|---|---|---|
| ε | Emissivity | - |
| h | Efficiency | - |
| ρ | Mass density | $kg/m^3$ |
| μ | Dynamic viscosity | Pa.s |
| s | Stefan-Boltzmann constant ($5{,}68\ 10^{-8}$) | $W/m^2.\ K^4$ |

**Subscripts**

| | |
|---|---|
| o | Initial |
| C | Compressor |
| CC | Bearing housing |
| ext | Extern |
| F | Friction |
| H | Oil |
| I | Inlet |
| IS | Isentropic |
| m | Mechanical |
| nc | Natural convection |
| O | Outlet |
| PCI | Inertia concentration point |
| rad | Radiation |
| sur | Surroundings |
| T | Turbine |
| u | Relative to the rotational speed |
| w | Wall |

**Appendix**

| | | unit | value |
|---|---|---|---|
| a | Friction Constant Eq. ( 7) | (-) | -0.5011 |
| b | Friction Constant Eq. ( 7) | (-) | $2.4016x10^{-10}$ |
| c | Friction Constant Eq. ( 7) | (-) | 2.54895 |
| $\varepsilon_T$ | Compressor emissivity | (-) | 0.64 |
| $\varepsilon_C$ | Turbine emissivity | (-) | 0.93 |
| $\varepsilon_{cc}$ | Main body emissivity | (-) | 0.93 |
| $Dext_C$ | Compressor wheel extern diameter | mm | 46.5 |
| $L_C$ | Compressor wheel width at outlet | mm | 2.5 |
| $Dext_T$ | Turbine wheel extern diameter | mm | 38.5 |
| $L_T$ | Turbine wheel width at inlet | mm | 6.1 |

**References**


Baar, R., Lucking, M., Sievert, M., 2005, *Die Turboladermodellierung für Prozessrechnungen bei erweiterter Leitungsbilanz*, Motor-prozessimulation und Aufldung, Berlin

Bohn, D., 2003a, "Conjugate Flow and Heat Transfer Investigation of a turbocharger Part II: Experimental Results", *ASME Conference Paper* GT2003-38449

Bohn, D., 2003b, "Conjugate Calculation of Flow Field and Heat Transfer in Compressor, Turbine and Casing of a Gas turbine", *VGB Powertech*, Vol.83, No.11, pp. 54-59

Bohn, D., Heuer, T., Kusterer, K., 2005, "Conjugate Flow and Heat Transfer Investigation of a Turbo Charger", *ASME Journal of Engineering for Gas Turbines and Power* Vol.127, pp. 663-669

Busam, S., Glahn, A., Witting, S., 2000, "Internal Bearing Chamber Wall Heat Transfer as a Function of Operating Conditions and Chamber Geometry", *ASME Journal of Engineering for Gas Turbines and Power*, Vol.122

Chapman, K.S., Nguru, R., Schultz, J., 2002, "Simplified Methodology to Correct Turbocharger Field Measurements for Heat Transfer and Other Effects", *Topical Report*, Kansas State University National Gas Machinery Lab.

Cormerais, M., Hetet, J.F., Chesse, P., Maiboom, A., 2006a, "Heat Transfer Analysis in a Turbocharger Compressor: Modeling and Experiments", *Paper presented at the SAE World Congress 2006*, April 3-6, Detroit, Michigan • USA

Cormerais M., Hetet J.F., Chesse P., Maiboom A., 2006 b, "Heat Transfers Characterisations in a turbocharger: experiments and correlations" *Proceedings of ICE 2006 : ASME Internal Combustion Engine Division 2006 Spring Technical Conference*, May 8 – 10, 2006 Aachen, Germany.

Cormerais, M., 2007, "Caractérisation expérimentale et modélisation des transferts thermiques au sein d'un turbocompresseur automobile. Application à la simulation du comportement transitoire d'un moteur Diesel à forte puissance spécifique", *Ph.D. Thesis of Ecole Centrale de Nantes.*

Depcik, C., Assanis, D., 2002, "A universal Heat Transfer Correlation for Intake and Exhaust Flows in a Spark-Ignition Internal Combustion Engine", *SAE paper 2002-01-0372*.

Descombes, G., 1996, "Contribution à l'étude des performances d'une petite turbine de suralimentation à géométrie variable", *Ph.D. Thesis, Paris VI University France.*

Esteco, 2009, ModeFrontier, http://www.esteco.com/

Gayvallet, H., Papchristos, G., Jullien, J., 1987, "Modélisation d'une Turbine Centripète de Suralimentation", Vol.23, No. 134, pp.19-26

Guzovic, Z., Matijasevic, B., Rusevljan, M., 2001, "Generalized Correlations for Heat Transfer Determination in Turbine Cascades", *Strojniski Vestnik*, Vol.47, No.8.

Hagelstein,D., Hasemann, H., Baar, R., Rautenberg, M., "Non-Adiabatic Energy Process in Exhaust Gas Turbines Using Heuristic Simulation Method", 1999, *Proceedings of the international Gas Turbine Congress*, Kobe.

Jones, T.V., 1991, "Definition of heat transfer coefficients in the turbine situation", *ImechE Paper* C423/046

Jung, M., Ford, R.G., Glover, K., Collings, N., Christen, U., Watts, M.J., 2002, "Parameterization and Transient Validation of a Variable Geometry Turbocharger for Mean-Value Modelling at Low and Medium Speed-Load Points", *SAE Paper 2002-01-2729.*

Jung, M., "Mean-Value Modelling and Robust Control of the Airpath of a Turbocharged Diesel Engine", 2003, *Degree of Doctor of Philosophy Cambridge College.*

Khalid, S.J., Hearne, R.E., 1980, "Enhancing Dynamic Model Fidelity for Improved prediction of Turbofan Engine Transient Performance", *AIAA*, 80-1083

Lallemand, A., 1983, "Modélisation d'un groupe turbocompressé de suralimentation de moteur alternatif", *Entropie*, 111.

Larjola, J., 1982, "Transient Simulation of Gas Turbines Including the Effects of Heat Capacity of the Solid Parts", PhD thesis, *Helsinki University of Technology, Laboratory of Aerodynamics.*

Moreno-Salas, N., 2006, "Modélisation des échanges thermiques dans une turbine radiale", *Thèse de doctorat Ecole Nationale Supérieure des Arts et Métiers*.

Podevin, P., Toussaint, M., Richard, G., Farinole, G., 2002, "Performances of turbocharger at low speed", *Ciepline Maszyni Przeplyowe Turbomachinery*, no: 122.

Pucher, H., Nickel, J., Sens, M., Grigoriadis, P., 2005, "Einfluss des Sensorik und der Messstellen-anordnung bei der Kennfeldvermessung und im Fahrzeugeinsatz von Turboladern", *Tagungsband* 10. Aufladetechnische Konferenz*,* 22.-23. Sept. 2005, Dresden, S. 285-305

Rautenberg, M., Kammer, N., 1984, "On the Thermodynamics of Non Adiabatic Compression and Expansion Process in Turbomachines", *Proceedings of the 5th International Conference for Mechanical Power Engineering, Cairo, Egypt.*

Rautenberg, M.,.Mobarak, A, Molababic, M., 1986, "Influence of heat transfer between turbine and compressor on the performance of small turbochargers", *JSME Paper 83-Tokyo-IGTC-73, International Gas Turbine Congress.*

Riegler, C., 1999, "Correlations to include heat transfer in gas turbine performance calculations", *Aerospace and Technology*, no: 5, 281-292.

Sacadura, J.F., 1993, "Initiation aux Transferts Thermiques, Centre d'actualisation scientifique et technique", *INSA de Lyon.*

Senechal, P., 1994, "Dimensionnement des Turbomachines", *SUPAERO département propulsion*, ISBN 2-84088-016-4.

Shaaban, S., 2004, "Experimental investigation and extended simulation of turbocharger non-adiabatic performance", *Doktor-Ingenieur Dissertation, Université de Hannover.*

Shaaban, S., Seume, J.R., 2006, "Analysis of Turbocharger Non-adiabatic Performance", *ImechE Turbocharger and Turbocharging.*

Younes, R., 1993, "Elaboration d'un modèle de connaissance d'un moteur diesel avec turbocompresseur à géométrie variable en vue de l'optimisation de ses émissions", *Thèse de doctorat Ecole Centrale de Lyon.*